Evidence of spin-wave demagnetization in Fe–Cr giant magnetoresistance multilayers

R. S. Patel and A. K. Majumdar[a)]
Department of Physics, Indian Institute of Technology, Kanpur-208 016, India

A. F. Hebard
Department of Physics, University of Florida, Gainesville, Florida 32611

D. Temple
MCNC, Electronic Technologies Division, Research Triangle Park, North Carolina 27709

(Received 20 September 2004; accepted 18 November 2004; published online 18 January 2005)

The temperature dependence of the saturation magnetization of Xe ion-beam sputtered Fe–Cr multilayers has been measured between 5 and 300 K in the presence of a field greater than the saturation field (H_{sat}). With the application of H_{sat}, the zero-field antiferromagnetically coupled ferromagnetic Fe layers are forced to align ferromagnetically. We find that the thermal demagnetization of such magnetically composite structure follows the Bloch formula for spin waves with anharmonic term in the magnon dispersion relation, viz., $M(T)=M(0)[1+AT^{3/2}+BT^{5/2}]$. Comparisons are presented between the multilayers and bulk crystalline Fe. © *2005 American Institute of Physics*. [DOI: 10.1063/1.1847720]

I. INTRODUCTION

Layered magnetic structures with alternate magnetic and nonmagnetic layers have drawn attention of researchers because of the rich physics involved as well as their much higher magnetoresistance compared to those showing anisotropic magnetoresistance effect (AMR). These multilayers are called giant magnetoresistance (GMR) materials. They are now gradually replacing the AMR materials in a variety of applications as magnetic read heads and hard-disk drives. Several Fe–Cr bilayers consisting of a few angstrom thick Fe and Cr layers have a tailor-made antiferromagnetic coupling between the ferromagnetic Fe layers (typically 20 Å) if the intervening Cr layer thickness ~10 Å. An external magnetic field completely aligns the spins of each Fe layer beyond a saturation field ($H_{sat}\sim 1$ T) forming a ferromagnetic arrangement causing a large drop in the electrical resistance.[1] Here we are presenting the temperature dependence of the saturation magnetization of Fe(20 Å)/Cr(t Å), $t=10$, 12 Å, in the range of 5–300 K, which is well below the Curie temperature (1043 K) of bulk Fe. These multilayers show a GMR of ~20% at 4.2 K at $H_{sat}\sim 1$ T. At any temperature GMR is a function of magnetic field but becomes field independent beyond H_{sat}. GMR is defined as $\mathrm{GMR}=((\rho(H,T)-\rho(0,T))/\rho(0,T))\times 100\%$. GMR properties of these multilayers have been studied at length.[1] It has been found that the magnetizations of thin films differ from those of the bulk. Although in the presence of a saturation field the Fe layers are aligned ferromagnetically, nevertheless, they have antiferromagnetic Cr (having negligible net moment) layers between them. The important question to ask is whether the composite arrangement (for $H>H_{sat}$) behaves as a bulk ferromagnet or not. Magnetization measurements as a function of temperature should throw some light on this important question.

Lindner *et al.*[2] found the temperature dependence of the interlayer exchange coupling between the ferromagnetic layers (through nonmagnetic spacers) as $J_{inter}\sim T^{3/2}$ by ferromagnetic resonance technique in Ni/Cu/Co and Ni/Cu/Ni trilayers and Fe_2V_5 multilayers; prepared by electron-beam evaporation. Rüdt *et al.*[3] observed in Fe_2V_5 multilayers that 2 monolayers (ML) of Fe behave as two-dimensional Ising-type all the way down without any dimensional crossover. The hyperfine magnetic field (from CEMS) showed a bulk-like $T^{3/2}$ dependence in epitaxial Fe films of thickness 7–40 Å deposited on W in the work of Korecki *et al.*[4] Bayreuther and Lugert[5] found that Fe films sandwiched between Ag are flat and continuous over distance >1000 Å, if its thickness is more than 3 atomic layers. Both bulk magnetization and Mössbauer data (CEMS) had shown that $M(T)\simeq AT^{3/2}$ and the higher order terms like $T^{5/2}$ were not detectable in magnetization even with a superconducting quantum interference device (SQUID) magnetometer because of the very small Fe mass. In a later paper Lugert and Bayreuther[6] reported in 4 ML of Fe (110) film grown epitaxially on Ag (111) substrate film that A (from Ms down to 2 K) $=(20\pm 1.5)\times 10^{-6}$ $K^{-3/2}$ and A (from CEMS down to 80 K) $=(22.5\pm 2)\times 10^{-6}$ $K^{-3/2}$ as against $A_{\mathrm{bulk\ Fe}}(Ms)=(5.0\pm 0.1)\times 10^{-6}$ $K^{-3/2}$, indeed a large enhancement for thin films. The values of A from CEMS (down to 90 K) are 21.6, 13.5, 9.5, 7.8×10^{-6} $K^{-3/2}$ for 3.4, 5.3, 8.6, 20.5 ML,[4] respectively. The effect of interface roughness leading to frustration and the antiferromagnetism of Cr itself affecting the temperature dependence of the interlayer coupling have been dealt by Pierce *et al.*[7] The critical spanning vectors of the Fermi surface of the Cr spacer layer determine the period, the asymptotic decay, and the temperature dependence of the oscillatory coupling as shown by Edwards *et al.*[8] and dis-

a)Electronic mail: akm@iitk.ac.in

cussed by Stiles.[9] Camley[10] gave detailed theories of spin-wave excitations in bulk and thin ferromagnetic films, multilayers with dipolar or exchange coupling, ultrathin films and multilayers and finally in antiferromagnets.

II. EXPERIMENTAL DETAILS

Fe–Cr multilayers of composition Si/Cr(50 Å)/[Fe(20 Å)/Cr(t Å)]$\times$30/Cr(50$-t$ Å) where t=10 and 12 Å were grown on Si substrates by ion-beam sputter deposition technique using Xe ions at 900 V and a beam current of 20 mA. These samples are well characterized and the details have been given elsewhere.[1] Sample 1 has a Cr thickness of t=10 Å and samples 2 and 3 have t=12 Å but they are deposited under different base pressure.

The temperature dependence of the saturation magnetization between 5 and 300 K of these multilayers was measured in a field of the order of 1 T ($>H_{\text{sat}}$). The magnetic field is applied in the plane of the multilayers. Measurements were carried out mainly at IIT Kanpur with a Quantum Design SQUID magnetometer (MPMS) with the standard dc transport head. Some measurements were also repeated at University of Florida. It should be mentioned here that the samples were loaded in the sample holder (straw) of MPMS without any packing material or tape or the capsule provided by Quantum Design. We found, through several test runs of $M(H,T)$, that using any of the above produces spurious additional positive moment $M\sim10^{-4}$ emu falling as $1/T$ below 20 K and fields of the order of 1 T. Even the very small paramagnetic contribution from the straw itself was subtracted out by measuring $M(T)$ of the straw alone from 5 to 300 K at 1 T. We have also measured the diamagnetic contribution from the Si substrate. It is linear in field and is almost independent of temperature. It is found to be of the order of 10^{-4} emu/T for a typical sample of (6 mm $\times$4 mm) area.

Instead of relying on the "literature data" for bulk Fe[11,12] we have measured $M(T)$ in two pieces (2.8 and 4.5 mg) of Specpure (Johnson—Matthey) Fe under identical conditions to those of the $M(T)$ measurements of our multilayers.

III. THEORY

The low-temperature (well below Curie temperature) magnetization of a typical crystalline ferromagnet is in good approximation explained by the spin-wave theory. For wave vector $\kappa\rightarrow0$, the dispersion relation of spin waves is given by[13,14]

$$\varepsilon(\kappa)=g\mu_B H_i+D\kappa^2+E\kappa^4+\cdots, \tag{1}$$

where ε is the energy of spin-wave excitations. The first term ($g\mu_B H_i\ll D\kappa^2$) of Eq. (1) represents an energy gap in the magnon spectrum arising from an effective internal field

$$H_i=H_{\text{applied}}-NM_s, \tag{2}$$

where H applied is the externally applied magnetic field and N is the demagnetization factor. In the present case we have taken N=0 since the magnetic field is in the plane of the film. So

$$H_i=H_{\text{applied}}. \tag{3}$$

In Eq. (1), D is the spin-wave stiffness constant and E is a proportionality constant. In the low-temperature limit, according to the Heisenberg model, the change in the spontaneous magnetization due to the excitation of spin waves can be written as[13]

$$M(T)=M(0)\left[1+Az\left(\frac{3}{2},\frac{T_g}{T}\right)T^{3/2}+Bz\left(\frac{5}{2},\frac{T_g}{T}\right)T^{5/2}\right], \tag{4}$$

where $M(0)$ is the magnetization at 0 K. $T_g=g\mu_B H_i/k_B$ is the gap temperature, $z(3/2,T_g/T)$ and $z(5/2,T_g/T)$ are the correction terms which reduce to unity if the effective internal magnetic fields vanish. These are given by[11]

$$\begin{aligned} z\left(\frac{3}{2},\frac{T_g}{T}\right)&=\frac{1}{2.612}\sum_{n=1}^{\infty}n^{-3/2}\exp\left[-\frac{nT_g}{T}\right]\\ &\approx\frac{1}{2.612}\left\{-3.54\left(\frac{T_g}{T}\right)^{1/2}+2.612\right.\\ &\quad\left.+1.46\frac{T_g}{T}-0.104\left(\frac{T_g}{T}\right)^2+\cdots\right\}, \end{aligned} \tag{5}$$

and

$$\begin{aligned} z\left(\frac{5}{2},\frac{T_g}{T}\right)&=\frac{1}{1.341}\sum_{n=1}^{\infty}n^{-5/2}\exp\left[-\frac{nT_g}{T}\right]\\ &\approx\frac{1}{1.341}\left\{-2.36\left(\frac{T_g}{T}\right)^{3/2}+1.341\right.\\ &\quad\left.-2.61\frac{T_g}{T}-0.730\left(\frac{T_g}{T}\right)^2+\cdots\right\}. \end{aligned} \tag{6}$$

In Eq. (4) the $T^{3/2}$ term comes from the harmonic term (κ^2) in the spin-wave dispersion relation [Eq. (1)] and the $T^{5/2}$ term comes from the anharmonic term (κ^4). Here, the coefficient A is related to D and given by

$$D=\frac{k_B}{4\pi}\left(\frac{2.612g\mu_B}{M(0)A}\right)^{2/3}. \tag{7}$$

The thermal demagnetization process of ferromagnetic metals at low temperatures ($T\ll T_C$) can be explained by both localized[15] and itinerant[16] models. In the localized model, electrons are localized to the atomic site. Interaction between these intra-atomic electrons determines the magnetization. Spin waves are excited at finite temperatures and in the process the magnetization decreases with T according to Eq. (4). In the itinerant model electrons move in the average field of other electrons/ions. In the low-temperature limit, thermal excitation of itinerant electrons from majority spin to the minority spin band, with increasing temperature, also results in thermal demagnetization. This is the so-called Stoner single-particle excitations. Bulk Fe and Co are weak ferromagnets. Here the density of states at the Fermi level for both the spin-up and spin-down bands are finite. For weak ferromagnets the Stoner term $\sim T^2$. Including the spin-wave $T^{3/2}$ term [of Eq. (4)], the net magnetization is given by

$$M(T)=M(0)[1+AT^{3/2}+\alpha T^2], \tag{8}$$

where α is a proportionality constant.

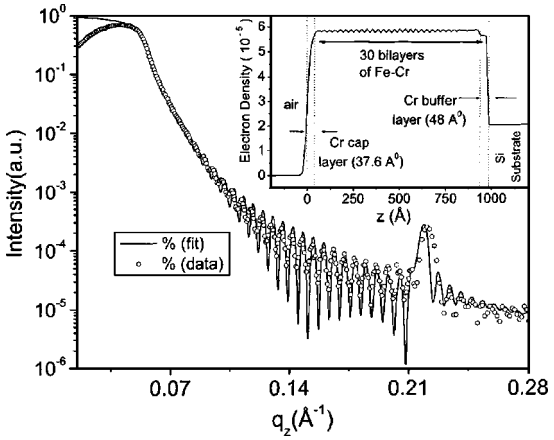

FIG. 1. The scattered small-angle x-ray intensity is plotted against $q_z(=4\pi \sin\theta/\lambda)$, the wave-vector transfer perpendicular to the surface. The fitting of the reflectivity curve is done by simulations based on Parratt's theory. The inset shows electron density against the depth measured from the top (opposite to Si substrate). The sharpness of the interfaces is quite obvious.

IV. RESULTS AND DISCUSSION

The GMR structures produced by our ion-beam sputter deposition system are comparable with the best structures fabricated using sputtering techniques, like ion-beam, dc-magnetron, etc. The quality of the multilayer structures was investigated by specular x-ray reflectivity measurements. This experiment was performed using a powder x-ray diffractometer (Siemens, Model D5000) with Cu $K\alpha$ radiation. A typical reflectivity profile, obtained for sample 3, is shown in Fig. 1. Here the normalized scattered intensity is plotted against q_z $(=4\pi \sin\theta/\lambda$, λ being the wavelength of the incident radiation), the wave-vector transfer perpendicular to the surface. The presence of sharp oscillations and huge variations in the magnitude (five orders) of the intensity over a large range of q_z strongly suggest the existence of well-defined interfaces within the layered structure. The fitting of the reflectivity data is done by simulations (using PARRATT32 software) based on Parratt's theory.[17] From the simulations, the average Fe thickness is found to be (18.4±0.1) Å (nominal value 20 Å), the Cr thickness (11.4±0.1) Å (nominal value 12 Å), and the rms interface roughness ~(6.5±0.5) Å. Here the definition of the rms roughness at the interface is the usual one as described in the literature.[18] The interface roughness and thickness fluctuations are essentially two independent parameters in the analysis of layered structures. The magnitude of the rms roughness could be smaller or larger than the actual layer thickness depending on how smooth or rough the overall surface is. The inset of Fig. 1 shows the electron density against the depth measured from the top (opposite to Si substrate). The sharpness of the interfaces is quite obvious.

Figure 2 shows M vs T data (points) for all the three samples from 5 to 100 K at their respective H_{sat}. $\Delta M/M$ is only ~0.9% over this 100 K change in temperature. The high resolution of the SQUID magnetometer makes such observations possible. We have calculated $z(3/2)$ and $z(5/2)$ and shown them in Fig. 3. Both $z(3/2)$ and $z(5/2)$ are smaller at lower temperatures implying larger corrections

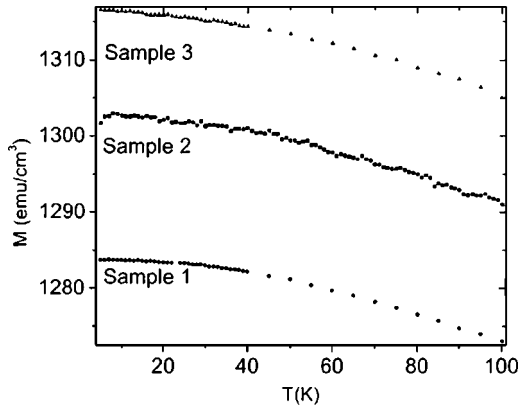

FIG. 2. Magnetization vs temperature plot for all three samples. The data of sample 3 are multiplied by 0.9. $\Delta M/M$ changes by *only* 1% between 5 and 100 K and by 5% between 5 and 300 K (not shown).

[for no correction both $z(3/2)$ and $z(5/2)=1$]. Also at all temperatures the $z(3/2)$ correction is more than the $z(5/2)$ and the correction at higher fields is always higher. For example, the correction, which is actually $1-z(3/2)$, is 25% at H_{sat} and 35% at $2H_{sat}$. $1-z(5/2)$, on the other hand, are 7% and 12%, respectively at H_{sat} and $2H_{sat}$.

Keeping in mind the above-mentioned features of the gap correction we have fitted the data for all three samples only at their respective H_{sat} (minimum correction) to Eq. (4) using a three-parameter least-squares fit program. We have restricted the fitting only up to 100 K since Eq. (4) is valid for $T \ll T_c$. Excellent fits were obtained for all three samples with correlation coefficients (R^2) of ~0.997 and values of the normalized

$$\chi^2\left(\chi^2 = \frac{1}{N}\sum_{i=1}^{i=N}\left(\frac{(M(\mathrm{raw})_i - M(\mathrm{fitted})_i)^2}{(M(\mathrm{raw})_i)^2}\right)\right)$$

consistent with the experimental resolution of 1 part in 10^4. The values of χ^2, R^2, $M(0)$, A, and B of Eq. (4) along with D of Eq. (7) are given in Table I for all the samples. Figure 4 shows M vs T plot for sample 2 (dots) along with the best fit to Eq. (4) (solid line). The % deviation in M of the data from the best-fitted curve $((M_{raw}-M_{fit})/M_{raw})\times 100\%$ is also

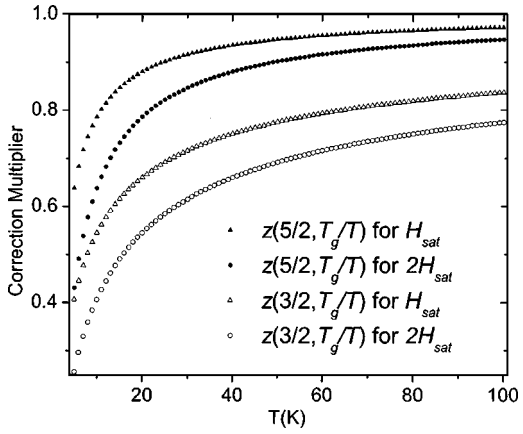

FIG. 3. The correction multipliers are plotted at every 1 K (between 5 and 100 K) for external magnetic fields of H_{sat} and $2H_{sat}$. It is clear that the corrections at low temperatures are more important. For no correction both $z(3/2)$ and $z(5/2)=1$.

TABLE I. Sample designation, value of χ^2, correlation coefficient (R^2), the best-fit coefficients M_0, A, and B of Eq. (4) along with D of Eq. (7).

Sample	$\chi^2(10^{-8})$	R^2	M_0(emu/cm^3)	$A(10^{-6}$ K$^{-3/2})$	$B(10^{-8}$ K$^{-5/2})$	D(meV Å^2)
Sample 1	1.19	0.9977	1283.9±0.1	−5.4±0.4	−4.3±0.4	213±13
Sample 1	5.12	0.9901	1284.3±0.1	−10.1±0.1	No term	⋯
Sample 2	4.12	0.9947	1302.9±0.1	−8.8±0.5	−1.8±0.4	152±11
Sample 2	4.92	0.9936	1303.1±0.1	−10.9±0.1	No term	⋯
Sample 3	0.62	0.9988	1462.8±0.1	−7.3±0.3	−2.4±0.3	160±7
Sample 3	1.83	0.9963	1463.0±0.1	−10.0±0.1	No term	⋯
Fe[a]	⋯	⋯	1731	−3.4±0.2	−0.1±0.1	289±15
Fe[b]	0.15	0.9987	1699.5±0.2	−3.90±0.05	No term	267±5

[a]Reference 11.
[b]Present investigation.

shown. The fit to Eq. (4) including the $T^{5/2}$ term is excellent. Not only are the deviations very small ($<0.02\%$), they are also quite random. It is observed from Table I that the values of the coefficient of the $T^{3/2}$ term, viz. A, averaged over all three samples $[(7\pm2)\times10^{-6}$ K$^{-3/2}]$ is twice as large as that of bulk crystalline Fe, found from Ref. 11 and our own SQUID measurements (details follow) on Specpure Fe samples. Nevertheless, it is of the same order. If we fit the above-mentioned data to Eq. (4) without the $T^{5/2}$ term, we get $A=(10.0\pm0.1)\times10^{-6}$ K$^{-3/2}$ averaged over all three samples. One should note here that our Fe–Cr multilayers have Fe thickness of 20 Å$\simeq$7 ML and it is quite consistent that our A values $(7\times10^{-6}$ K$^{-3/2})$ are between those of the bulk $(3.5\times10^{-6}$ K$^{-3/2})$[11] and the 4 ML of Fe $(20\times10^{-6}$ K$^{-3/2})$[6]. Also, it compares very well with 9.5×10^{-6} K$^{-3/2}$ for 8.6 ML of Korecki *et al.*[4] as described in Sec. I. The coefficient of the $T^{5/2}$ term, viz. B, which is due to the anharmonicity in the magnon dispersion relation, comes out to be ~30 times[11] as large $[(3\pm1)\times10^{-8}$ K$^{-5/2}]$. This may be due to the Cr spacer layer introducing significant anharmonicity for the spin waves.

Camley[10] found that in magnetic multilayers if the ferromagnetic film thickness is greater than the thickness of the nonmagnetic spacer layer, then collective surface mode of spin waves exists. When the collective mode is composed of surface-type modes in each film, the solution turns out to be simple, it is just the dispersion relation for a semi-infinite ferromagnet. It almost appears as if the layering plays no role at all. In all our samples the ferromagnetic Fe layer thickness is more than that of the nonmagnetic Cr. Köbler[19] had mentioned that the three-dimensional properties disappeared completely for thin film Fe samples with less than only three atomic layers. Three layers are the absolute minimum for the realization of spin waves perpendicular to the thin film plane. In our samples the Fe layers have thickness of 20 Å, which is definitely much more than three atomic layers.

At this stage we present our data on crystalline Fe. Figure 5 shows magnetization versus temperature at an external field of 0.3 T (enough to reach saturation in that particular orientation) for three different runs of a Specpure Fe sample. However, we observed that the linear thermal expansion coefficient of Fe changes from 0.17 to 46×10^{-7} K^{-1} from 5 to 100 K[20] leading to a volume change of 0.06% of the sample. This introduces significant error in the magnetization of pure Fe where the magnetic moment changes by only 0.32% from 5 to 100 K. We have calculated the volume change at each temperature (by proper integration) and corrected the magnetization value at the corresponding temperature. The points in Fig. 5 represent the data after the thermal expansion correction has been applied. Now, $\Delta M/M$ changes by 0.38% between 5 and 100 K. We find that the corrected

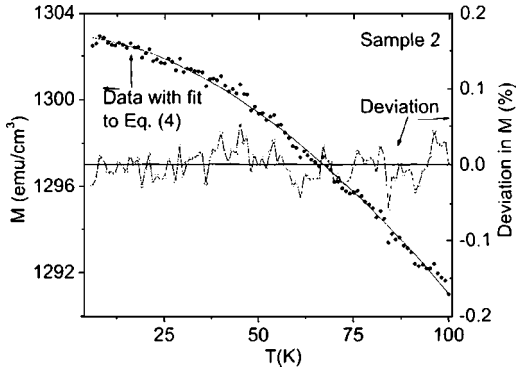

FIG. 4. Magnetization vs temperature plot for sample 2. The dots represent the data points and the solid line is the fit to Eq. (4). The deviation in M of the raw data from the best-fitted curve $((M_{raw}-M_{fit})/M_{raw})\times100\%$ is also plotted against T. It is less than 0.02%.

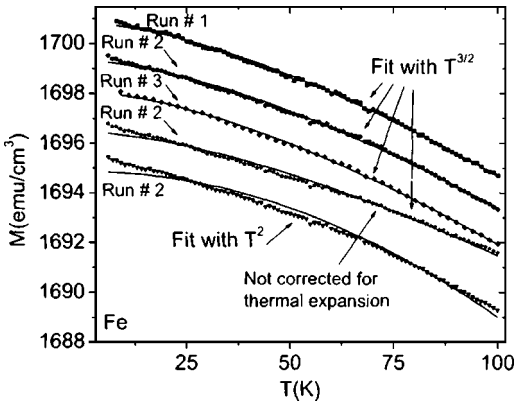

FIG. 5. Magnetization vs temperature plot for three different runs of Specpure Fe sample. $\Delta M/M$ changes by *only* 0.38% between 5 and 100 K. The dots represent the data points after the thermal expansion correction and the solid lines are the best fits to Eq. (4). The data and the fits for run 2 without the correction and to a single power T^2 relation are also shown for comparison. Some data are shifted in magnetization axis for clarity.

data fit very well with Eq. (4) but with only the $T^{3/2}$ term with χ^2 values consistent with the experimental resolution, correlation coefficient of 0.999 and the coefficient $A=(3.90\pm0.05)\times10^{-6}$ $K^{-3/2}$, averaged over the three independent runs. The best-fitted curves are shown in Fig. 5 as solid lines. This result is not too different from that of Argyle *et al.*[11] [$(3.4\pm0.2)\times10^{-6}$ $K^{-3/2}$]. We could not isolate the $T^{5/2}$ term although the resolution of our SQUID measurements is 10 times better for Fe (mass ~4.5 mg) than those for the multilayers (1 part in 10^4). Although Argyle *et al.*[11] had definitely established the $T^{3/2}$ term, they could not find the $T^{5/2}$ term conclusively because of 100% error in the coefficient $D=(0.1\pm0.1)\times10^{-8}$ $K^{-5/2}$, in spite of the fact that their resolution (1 part in 10^6) is much better than most reported later (1 in 10^4), including ours (1 in 10^5). Also, the possibilities of the itinerant electron term ST^2 and the thermal expansion term $E\Delta l(t)/l_0$ could not be ruled out.

Also included in Fig. 5 are the data and the fit for run 2 showing the importance of the thermal expansion correction.

Crangle and Goodman[12] found $M(T)$ varying as T^2 all the way to the lowest temperature in bcc bulk Fe. However, they had only 5 data points below 100 K and their accuracy was only 1 in 10^4. We actually plotted their data from the lowest temperature until 300 K and found that $n=1.88$ (single power). Our data on Fe (95 data points even below 100 K), plotted similarly until 300 K, gave $n=1.89\pm0.01$ but if the data are fitted only at low temperatures (5–100 K) Eq. (4) holds very well, i.e., the exponent is 3/2 and not 2. The motivation behind the present work is to see how $M(T)$ behaves for $T\ll T_C$ for both the Fe–Cr multilayers as well as for bulk Fe. We therefore consider data only below, say, 100 K. As elaborated above, the bulk Fe data fit much better to Eq. (4) (only with $T^{3/2}$ term) with $\chi^2=0.15\times10^{-8}$ and correlation coefficient=0.999 than to a single power T^2 (like that of Crangle and Goodman) with $\chi^2=1.35\times10^{-8}$, i.e., 9 times as much. In Fig. 5 we show the data of run 2 of Fe with a single power T^2 fit for comparison. So our $M(T)$ data for pure Fe below 100 K is nowhere close to a T^2 fit, as concluded by Crangle and Goodman from their data (too few below 100 K).

Köbler[19] has pointed out that it is more meaningful to fit $M(T)$ data of Fe to single-power laws (T^{ε}) with dimensional crossovers rather than the Dyson-type multiple-power law [Eq. (4)]. $\varepsilon=2$ for crystalline Fe and 3/2 for isotropic crystalline two-dimensional Fe films. Also, for 3 ML or more of ultrathin Fe films, there is a thermodynamic crossover from $T^{3/2}$ to T^2 at around 467 K. We could not find any such crossover in the range of our interest (until 100 K) in our Fe–Cr multilayers and Specpure bulk Fe samples. Experiments of Lugert and Bayreuther[5] do show three-dimensional behavior of Fe above 3 ML. Also, Korecki *et al.*[4] did not find any dimensional crossover until 300 K ($T^{3/2}$ to T^2 at higher temperatures) for 8.6 ML of Fe. To summarize, our multilayer samples with ≃7 ML of Fe behave more like bulk Fe (described in the last two paragraphs), both showing spin-wave excitations according to Eq. (4) with/without the Dyson $T^{5/2}$ term.

To check the presence of the $T^{5/2}$ term in the interpretation of $M(T)$ we fitted the data of all the multilayer samples

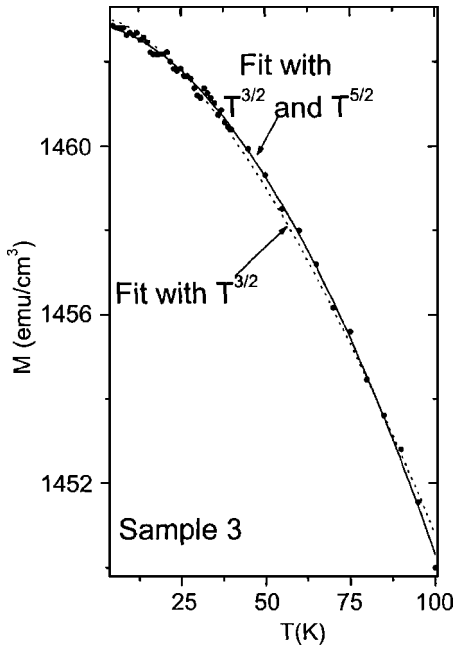

FIG. 6. Magnetization vs temperature for sample 3. The dots are the data points whereas the solid and dashed lines are the best-fitted curves as indicated.

to Eq. (4) but without the $T^{5/2}$ term. Figure 6 shows fits with (solid line) and without (dashed line) the $T^{5/2}$ term for comparison. It is obvious that the former fit is much better than the latter. Not only is the value of χ^2 higher by a factor of ~3 for the fits without the $T^{5/2}$ term, the deviation of the best-fitted curve from the experimental one is more and systematic whereas it is much smaller and, more important, quite random for the fit with the $T^{5/2}$ term as shown in Fig. 7. This observation of a $T^{5/2}$ term over and above the $T^{3/2}$ term in our Fe–Cr multilayers is much better seen in Fig. 8 where the $T^{3/2}$ fit until 100 K is extended to 300 K along with the data for all the samples. Needless to say the inclusion of the $T^{5/2}$-like term is necessary primarily at higher temperatures. We also observed that the thermal expansion correction had not changed any of our conclusions because of its relatively smaller magnitude in the case of the Fe–Cr multilayer samples.

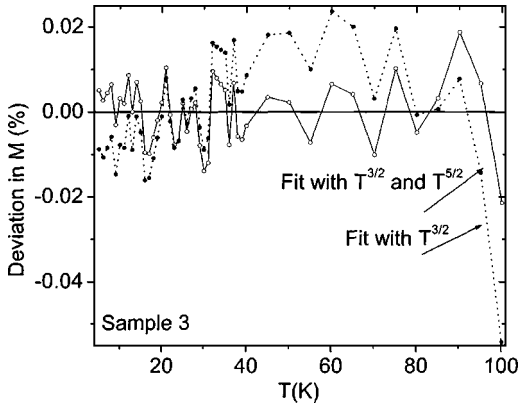

FIG. 7. The deviation in magnetization (M) of the raw data from the best-fitted curve is plotted against temperature for sample 3. The deviations are large and systematic for the fit with only the $T^{3/2}$ term whereas they are small (~0.005%) and rather random for the one including both $T^{3/2}$ and $T^{5/2}$ terms.

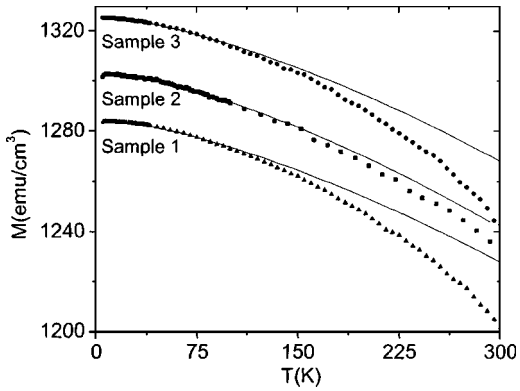

FIG. 8. Magnetization vs temperature for all three Fe–Cr multilayer samples. The fit to Eq. (4) without the $T^{5/2}$ term until 100 K is extended to 300 K (solid lines) along with the data. The necessity for the inclusion of the $T^{5/2}$-like term is quite evident at higher temperatures. The data and fit of sample 3 are multiplied by 0.906.

The spin-wave stiffness constant is found to be of the same order but less than that of bulk Fe. The value of D seems to decrease with the increase of Cr thickness ($\sim$210 and $\sim$155 meV Å^2 for $t=10$Å and 12Å, respectively). Wider variation of "t" might throw more light on this aspect of exchange coupling between the Fe layers through the Cr spacer layer. Thus for $H > H_{sat}$, so far as the thermal demagnetization is concerned, not only does the composite Fe–Cr multilayer system behave as a bulk crystalline ferromagnet but also it shows unequivocal evidence of the anharmonic term in the magnon spectrum.

We also tried to investigate the effect of external magnetic field above H_{sat} on the coefficients A and B. We repeated the experiment under the same conditions for external fields of $1.5H_{sat}$ and $2H_{sat}$. The coefficients are coming out to be independent of field within the above-quoted experimental errors for A and B averaged over the three samples. The gap corrections here are much larger than that for H_{sat}. Apart from this we tried to fit our data to Eq. (8) for weak ferromagnets to look for any evidence of Stoner excitations. However, we got unphysical value and sign of the coefficients.

To conclude, the thermal demagnetization has been studied in ion-beam sputtered Fe–Cr GMR multilayers. The decrease in magnetization with temperature is well explained in terms of Bloch's spin-wave theory. The power law dependence and the associated coefficients in these thin film multilayers are similar to those of pure Fe.

ACKNOWLEDGMENTS

R.S.P. acknowledges CSIR, Government of India for financial support. We also acknowledge Dr. Josh Kelly for his technical assistance in some measurements and P. Khatua for allowing us to use his unpublished work on small-angle x-ray scattering of our Fe–Cr multilayer samples.

[1] A. K. Majumdar, A. F. Hebard, A. Singh, and D. Temple, Phys. Rev. B **65**, 054408 (2002) and references therein.
[2] J. Lindner, C. Rüdt, E. Kosubek, P. Poulopoulos, K. Baberschke, P. Blomquist, R. Wäppling, and D. L. Mills, Phys. Rev. Lett. **88**, 167206 (2002).
[3] C. Rüdt, P. Poulopoulos, J. Lindner, A. Scherz, H. Wende, K. Baberschke, P. Blomquist, and R. Wäppling, Phys. Rev. B **65**, 220404 (2002).
[4] J. Korecki, M. Przybylski, and U. Gradmann, J. Magn. Magn. Mater. **89**, 325 (1990).
[5] G. Bayreuther and G. Lugert, J. Magn. Magn. Mater. **35**, 50 (1983).
[6] G. Lugert and G. Bayreuther, Phys. Rev. B **38**, 11068 (1988).
[7] D. T. Pierce, J. Unguris, R. J. Celotta, and M. D. Stiles, J. Magn. Magn. Mater. **200**, 290 (1999).
[8] D. M. Edwards, J. Mathon, R. B. Muniz, and M. S. Phan, Phys. Rev. Lett. **67**, 493 (1991).
[9] M. D. Stiles, J. Magn. Magn. Mater. **200**, 322 (1999).
[10] R. E. Camley, J. Magn. Magn. Mater. **200**, 583 (1999).
[11] B. E. Argyle, S. H. Charap, and E. W. Pugh, Phys. Rev. **132**, 2051 (1963).
[12] J. Crangle and G. M. Goodman, Proc. R. Soc. London, Ser. A **321**, 477 (1971).
[13] A. K. Majumdar, V. Oestreich, D. Weschenfelder, and F. E. Luborsky, Phys. Rev. B **27**, 5618 (1983).
[14] F. Keffer, in *Handbuch der Physik*, edited by S. Flügge and H. P. J. Wijn (Springer, Berlin, 1966), Vol. XVIII/2.
[15] W. Heisenberg, Z. Phys. **49**, 619 (1928).
[16] E. C. Stoner, Proc. R. Soc. London, Ser. A **154**, 456 (1936).
[17] L. G. Parratt, Phys. Rev. **95**, 359 (1954).
[18] M. Tolan, *X-ray Scattering from Soft-Matter Thin Films*, Springer Tracts in Modern Physics, Vol. 148 (Springer, Heidelberg, 1999).
[19] U. Köbler, J. Phys.: Condens. Matter **14**, 8861 (2002).
[20] G. K. White, Proc. Phys. Soc. London **86**, 159 (1965).